

SYNAPSE: Neuro-Symbolic Visual Thought-to-Text Decoding via Topological Semantic Denoising

Akshaj Murhekar

School of Information
University of Texas at Austin
akshaj.murhekar@utexas.edu

Abhijit Mishra

School of Information
University of Texas at Austin
abhijitmishra@utexas.edu

Abstract

Recent advances in large language models have accelerated open-vocabulary EEG-to-imagined-text decoding, where non-invasive neural activity recorded during visual perception is translated into coherent natural language descriptions of viewed stimuli. However, existing systems remain highly vulnerable to biological noise, where corrupted neural projections induce hallucinated or semantically unstable generation in frozen language models. We introduce SYNAPSE (Symbolic Neural Alignment for Precise Semantic Extraction), a lightweight neuro-symbolic framework that stabilizes neural text generation through inference-time symbolic regularization. By purifying EEG-derived semantic candidates using commonsense graph structure and latent exemplars, SYNAPSE improves semantic stability without end-to-end LLM fine-tuning. Experiments across popular EEG decoding benchmarks and multiple frozen LLM backends demonstrate consistent gains over unconstrained prompting baselines, robustness under object-label ablation, and performance commensurate with substantially more resource-intensive fine-tuned systems, while preserving biometric privacy by localizing raw EEG processing entirely within the encoder stack.

1 Introduction

Translating continuous neural recordings into natural language text has long remained a central objective at the intersection of computational neurotechnology and artificial intelligence. Recent advances in multi-modal generative deep learning have accelerated non-invasive brain-to-text decoding frameworks, particularly those leveraging electroencephalography (EEG) due to its temporal resolution, portability, and clinical feasibility (He et al., 2015; Benchetrit et al., 2023; Défossez et al., 2023). In parallel, the rapid evolution of large language models (LLMs) has introduced highly flexible reasoning systems capable of contextual alignment

across text, vision, and speech modalities (Touvron et al., 2023; Achiam et al., 2023), driving growing interest in continuous latent translation pipelines that bridge cortical activity and coherent linguistic generation for applications in assistive communication, immersive interfaces, and neurological healthcare. In particular, recent work has focused on **visual thought-to-text translation**, where EEG activity elicited during visual perception is decoded into natural language descriptions of viewed stimuli (Mishra et al., 2025; Murhekar et al., 2026). Early open-vocabulary approaches relied on **end-to-end fine-tuning** of autoregressive or encoder-decoder architectures directly on multi-channel neural recordings (Wang et al., 2024; Lamprou and Moshfeghi, 2025; Mishra et al., 2025); however, such tightly coupled training paradigms require substantial computational infrastructure, introduce **privacy risks** through exposure of sensitive biometric signals, and often suffer from poor generalization as downstream language models evolve. To address these limitations, recent decoupled frameworks such as SENSE replace continuous parameter optimization with **discrete latent alignment strategies** that project neural signals into a fixed vocabulary space, enabling frozen off-the-shelf LLMs to synthesize fluent text from candidate keywords in a zero-shot setting (Murhekar et al., 2026).

However, recent EEG-to-text systems remain constrained within a purely connectionist framework. Because scalp EEG recordings are highly susceptible to physiological artifacts, noisy latent projections often activate semantically unrelated candidate tokens alongside the true intent, a phenomenon we term topical incongruence. When injected directly into frozen LLM prompts, these corrupted semantic cues induce attentional dispersion and hallucinated generation. **This raises a fundamental question: can symbolic structure stabilize noisy neural semantic representations without retraining large language mod-**

els? To address this, we introduce SYNAPSE, a lightweight neuro-symbolic regularization framework that routes EEG-derived semantic candidates through a commonsense multigraph prior to decoding. A deterministic graph purification stage removes disconnected semantic noise where normalized degree centrality satisfies ($C_D(\mathbf{v}) = 0$), while preserving high-priority neural targets through a conditional union constraint. The framework further enriches decoding with grounded relational facts (\mathcal{F}) and latent syntactic exemplars ($\mathcal{E}_{\text{exemplars}}$) retrieved directly from neural embeddings ($\mathbf{S} = \mathbf{x} \cdot \mathbf{E}^\top$), producing a purified semantic context that stabilizes downstream language generation.

We evaluate SYNAPSE on two public EEG-to-language benchmarks: CVPR2017 (Spampinato et al., 2017) and THINGS EEG2 (Gifford et al., 2022; Wu et al., 2025), augmenting both datasets with image-grounded captions to support open-vocabulary neural text generation. Across a heterogeneous decoder suite spanning Meta-Llama-3-8B-Instruct, Qwen2.5-7B-Instruct, GPT-4o-mini, and Gemini-2.5-flash-lite, we conduct extensive evaluation using ROUGE, BLEU, METEOR, BERTScore, GPT-5 LLM-as-a-judge assessment, and systematic ablation analysis. Results on CVPR2017 show clear and consistent gains over unconstrained prompting and prior decoupled decoding baselines, particularly under aggressive object-label ablation where symbolic regularization substantially improves semantic stability and retrieval robustness. On the more challenging THINGS EEG2 benchmark, SYNAPSE achieves performance largely **commensurate** with or exceeding competitive neuro-symbolic and fine-tuned approaches across multiple metrics, while maintaining stronger cross-model consistency under noisy latent conditions. Unlike compute-intensive continuous training pipelines such as THOUGHT2TEXT (Mishra et al., 2025), our framework operates as a lightweight inference-time layer aligned with modern retrieval-augmented generative paradigms, enabling frozen LLM deployment while preserving biometric privacy since raw EEG signals remain localized to the encoder stack and never require external model adaptation. To summarize, our key contributions are as follows:

- We introduce SYNAPSE, a lightweight neuro-symbolic framework for inference-time

EEG semantic regularization without end-to-end LLM fine-tuning.

- We propose a graph purification mechanism that removes disconnected semantic noise while preserving high-confidence neural intent.
- We develop a latent exemplar retrieval strategy that injects syntactic templates to stabilize downstream generation under noisy biological conditions.
- We demonstrate robust and competitive decoding performance across multiple EEG corpora, frozen LLMs, and ablation settings.

The complete reproducibility package has been open-sourced at anonymous.4open.science/r/neuro-symbolic-eeg-to-text-26F2.

2 Related Work

Brain-computer interfaces (BCIs) for natural language decoding have rapidly evolved from discrete command classification to continuous brain-to-text generation. Early systems primarily relied on invasive neuroprostheses to decode handwriting and speech articulation from cortical recordings (Willett et al., 2023; Metzger et al., 2022), while subsequent work extended these paradigms to non-invasive settings, demonstrating reconstruction of perceived speech (Défossez et al., 2023), visual stimuli (Benchetrit et al., 2023), semantic narratives (Tang et al., 2023), and typing-based communication (Lévy et al., 2025). However, decoding natural language directly from EEG remains fundamentally challenging due to the low spatial resolution and high noise sensitivity of scalp recordings.

Recent EEG-to-text architectures address these limitations through cross-modal alignment and self-supervised representation learning. Prior work has explored contrastive masked autoencoders (Wang et al., 2024), large-scale neural pre-training (Lamprou and Moshfeghi, 2025), interpretable semantic alignment (Liu et al., 2025), and semantic matching frameworks for open-vocabulary generation (Tao et al., 2025; Masry et al., 2025). State-of-the-art systems such as THOUGHT2TEXT (Mishra et al., 2025) rely on resource-intensive end-to-end fine-tuning of autoregressive language models, while decoupled retrieval-based approaches such as SENSE (Murhekar et al., 2026) replace model adaptation with discrete vocabulary retrieval over frozen

LLMs. However, both paradigms remain fully connectionist and therefore vulnerable to physiological noise, latent representation drift, and downstream hallucinated generation. In contrast, SYNAPSE introduces an inference-time neuro-symbolic regularization framework that performs topological graph purification and relational grounding over EEG-derived semantic projections, stabilizing frozen language decoders without updating model parameters.

3 Methodology

SYNAPSE decodes continuous EEG recordings into natural language without requiring autoregressive LLM fine-tuning. While existing retrieval-based paradigms (Murhekar et al., 2026) propagate unconstrained latent noise that triggers semantic drift and hallucinations, our framework introduces a neuro-symbolic intervention layer (Figure 1) that systematically purifies neural latents. This is achieved via three core operations: graph-based knowledge grounding, relational fact assertion, and non-parametric exemplar retrieval, which together constrain the LLM generation footprint within a validated semantic manifold.

3.1 Problem Formulation and Neural Frontend Retrieval

Given paired trials $\mathcal{D} = \{(X_i, s_i)\}_{i=1}^N$, where $X_i \in \mathbb{R}^{C \times T}$ and s_i is the target caption, we adopt the frozen SENSE frontend (Murhekar et al., 2026). Raw signals X_i map to language-aligned latents $\mathbf{z}_i \in \mathbb{R}^{512}$ via a ChannelNet encoder and MLP refiner ($\sim 6\text{M}$ parameters). A candidate token set \mathbf{W}_{raw} is extracted using scale-normalized cosine similarity against a frozen vocabulary matrix \mathbf{V} :

$$\mathbf{W}_{\text{raw}} = \text{TopK} \left(\sigma \left(\frac{\mathbf{z}_i}{\|\mathbf{z}_i\|_2} \cdot \left(\frac{\mathbf{V}}{\|\mathbf{V}\|_2} \right)^\top \right), k = 15 \right) \quad (1)$$

This unpurified array \mathbf{W}_{raw} serves as the direct operational input for our subsequent neuro-symbolic purification layers.

3.2 Knowledge-Grounded Subgraph Induction and Topological Pruning

To regularize the prediction stream via external world knowledge, SYNAPSE projects candidate tokens into a common-sense repository (ConceptNet) (Speer et al., 2017), formalized as a weighted,

directed multigraph $\mathcal{K} = (\mathcal{V}_{\mathcal{K}}, \mathcal{E}_{\mathcal{K}}, \mathcal{W}_{\mathcal{K}}, \mathcal{R}_{\mathcal{K}})$ containing vertices $\mathcal{V}_{\mathcal{K}}$, edges $\mathcal{E}_{\mathcal{K}}$, confidence weights $\mathcal{W}_{\mathcal{K}}$, and relation types $\mathcal{R}_{\mathcal{K}}$. At inference time, the $k = 15$ candidate elements from \mathbf{W}_{raw} are projected into the graph to construct a target concept vertex set $V_G \subseteq \mathcal{V}_{\mathcal{K}}$. We extract a knowledge-grounded induced subgraph $G = (V_G, E_G)$ by enforcing a minimum edge-weight threshold $w_{\text{min}} = 1.0$:

$$E_G = \{(u, v) \in \mathcal{E}_{\mathcal{K}} \mid u, v \in V_G \wedge w(u, v) \geq w_{\text{min}}\} \quad (2)$$

To filter out spurious tokens, we evaluate node connectivity within G . For each vertex $v \in V_G$, we compute its normalized degree centrality $C_D(v) = \text{deg}(v)/(|V_G| - 1)$, where $\text{deg}(v)$ is the node degree within G . Rather than automatically dropping all isolated nodes where $C_D(v) = 0$, SYNAPSE implements a hybrid selection rule utilizing a neural priority safeguard set $P = \{w_i \in \mathbf{W}_{\text{raw}} \mid i \leq m\}$ (where $m = 5$). The final pruned vocabulary $\mathbf{W}_{\text{pruned}}$ supplied to the language decoder is defined by the conditional union:

$$\mathbf{W}_{\text{pruned}} = \{v \in V_G \mid C_D(v) > 0 \vee v \in P\} \quad (3)$$

This topological restriction deterministically regularizes connectionist prediction noise while preserving high-confidence fallback anchors.

3.3 Relational Fact Extraction for Context Grounding

To anchor downstream linguistic synthesis, SYNAPSE traverses the edge boundaries E_G of the extracted subgraph to harvest available semantic assertions. This traversal is restricted to a subset of visually relevant relationship types $\mathcal{R}_{\text{meaningful}} \subset \mathcal{R}_{\mathcal{K}}$ (e.g., *AtLocation*, *UsedFor*, *HasProperty*, *CapableOf*, *PartOf*). For each discovered directed edge possessing a label $r(u, v) \in \mathcal{R}_{\text{meaningful}}$, a rule-based mapping function $\tau(u, r, v)$ translates the abstract graph triple into a natural language string. The total discovered assertions are accumulated into an ordered candidate set $\mathcal{F}_{\text{all}} = \{\tau(u, r(u, v), v) \mid (u, v) \in E_G \wedge r(u, v) \in \mathcal{R}_{\text{meaningful}}\}$. To handle variable relational density and maintain prompt efficiency, we slice this sequence to a rigid capacity threshold $N_{\text{facts}} = 5$, yields the opportunistic context cache \mathcal{F} :

$$\mathcal{F} = \mathcal{F}_{\text{all}}[1 : N_{\text{facts}}] \quad (4)$$

Injecting \mathcal{F} into the final generation prompt provides the downstream decoder with explicit, struc-

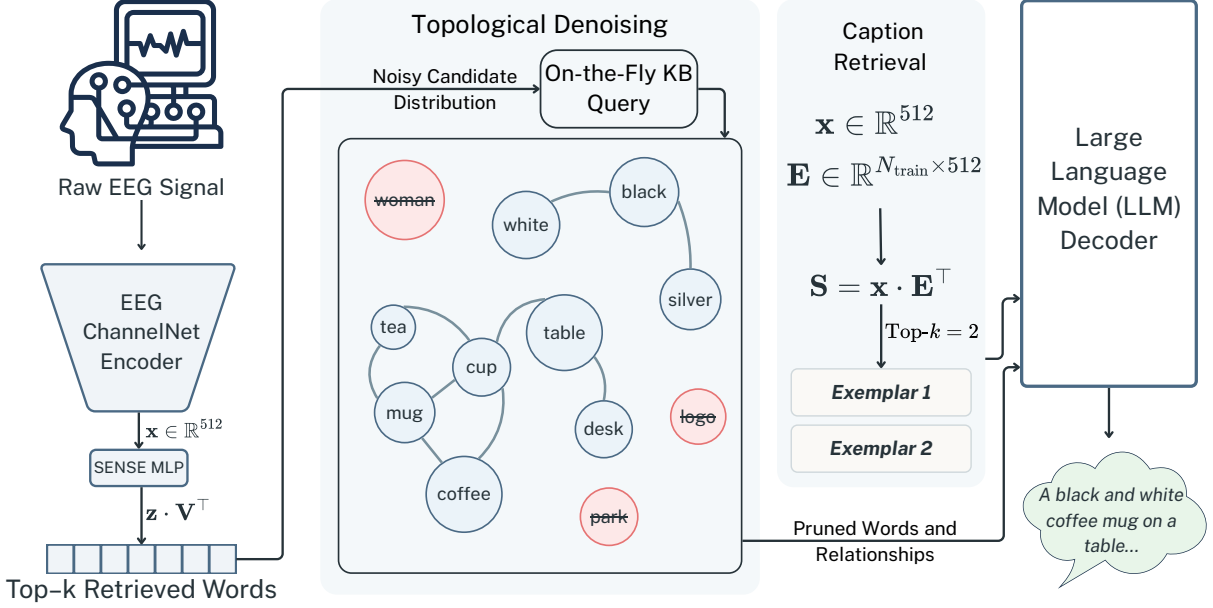


Figure 1: Overview of the SYNAPSE neuro-symbolic framework. Raw candidate keywords extracted from the baseline frontend via $\mathbf{z} \cdot \mathbf{V}^\top$ undergo topological graph purification to drop spurious singletons and harvest grounded relational facts. Concurrently, the unrefined neural latent vector \mathbf{x} queries a historical training matrix \mathbf{E} via parallel cosine similarity $\mathbf{S} = \mathbf{x} \cdot \mathbf{E}^\top$ to fetch nearest-neighbor syntactic blueprints. The purified vocabulary anchors, relational context, and structural templates are fused into a consolidated prompt to guide generation across a suite of frozen large language model (LLM) decoders.

turally validated common-sense constraints.

3.4 Cross-Modal Exemplar Retrieval for Syntactic Blueprinting

To supply the decoder with target syntactic templates without autoregressive fine-tuning, SYNAPSE implements a non-parametric, cross-modal exemplar retrieval strategy executed directly on the unrefined neural latent space. Let the historical training split index be represented by the frozen matrix $\mathbf{E} \in \mathbb{R}^{N_{\text{train}} \times 512}$ containing the stacked ChannelNet embeddings of historical trials. During inference, the active unrefined feature vector $\mathbf{x} \in \mathbb{R}^{512}$ serves as the continuous query. We compute a parallel cosine similarity score vector $\mathbf{S} \in \mathbb{R}^{N_{\text{train}}}$ via a single tensor operation:

$$\mathbf{S} = \mathbf{x} \cdot \mathbf{E}^\top \quad (5)$$

We isolate the indices of the nearest-neighbors via a strict selection rule where $\text{Top-k} = 2$. Their corresponding target natural language captions are retrieved from local storage to construct the syntactic exemplar set $\mathcal{E}_{\text{exemplars}}$.

3.5 Linguistic Decoding Loop

The final phase of SYNAPSE consolidates the extracted features into a structured prompt configuration. This unified prompt aggregates four distinct

data streams: (i) the topologically purified token sequence W_{pruned} , (ii) the grounded semantic prose facts \mathcal{F} , (iii) the cross-modal syntactic exemplars $\mathcal{E}_{\text{exemplars}}$, and (iv) a target visual object class anchor with static stylistic generation constraints. The consolidated prompt is routed through a frozen, off-the-shelf large language model (LLM) decoder to execute autoregressive generation at the edge.

4 Experiments

We evaluate the performance of SYNAPSE across varied benchmarks, language decoders, and translation fidelity criteria.

4.1 Experimental Setup and Datasets

THOUGHT2TEXT / SENSE Benchmark: We evaluate SYNAPSE on the multi-modal EEG-to-text benchmark corpus from (Mishra et al., 2025; Murhekar et al., 2026). This dataset features non-invasive EEG recordings from six healthy subjects viewing visual stimuli from ImageNet, paired with descriptive natural language captions. Following SENSE verbatim, raw neural features are encoded into 512-dimensional vector spaces via a frozen ChannelNet architecture using the default pipeline hyperparameters established in Section 3.

THINGS EEG2 Cross-Exemplar Suite: For open-vocabulary scaling, we evaluate SYNAPSE on the public THINGS EEG2 repository (Gifford et al., 2022). Because the original corpus lacks target textual descriptors, we adapt the data-bootstrapping paradigm introduced in THOUGHT2TEXT (Mishra et al., 2025) and employ a large language model (GPT-5.4-mini) to synthesize ground-truth text captions one-by-one for each visual stimulus across all 1,654 concepts. Our active experimental boundary isolates the first 5 healthy subjects. Moving beyond standard concept-disjoint splits, we enforce a strict cross-exemplar evaluation: the training matrix uses exclusively averaged EEG responses from the first 5 unique image exemplars per concept, whereas the test split targets the responses to a completely unseen 6th image exemplar within the matching concept channel (1,654 total pooled test samples). For both splits, deterministic cross-trial averaging is executed over the 4 repetitive presentation epochs to maximize the biological Signal-to-Noise Ratio (SNR).

4.2 Evaluated Decoders and Metrics

We route our consolidated prompts through a diverse suite of large language model decoders, spanning open-weights architectures—Qwen2.5-7B-Instruct and Meta-Llama-3-8B-Instruct—and commercial endpoints—GPT-4o-mini and Gemini-2.5-flash-lite, all available via API access. Following the established evaluation protocols of Thought2Text (Mishra et al., 2025) and contemporary baselines (Murhekar et al., 2026), translation fidelity is evaluated using standard lexical overlap metrics: BLEU-1/4 (Papineni et al., 2002), ROUGE-1/2/L (Lin, 2004), and METEOR (Banerjee and Lavie, 2005). We complement these string-matching protocols with continuous vector matching via BERTScore (Zhang et al., 2019), along with an automated LLM-as-a-judge framework to evaluate text fluency and adequacy on a standardized 1–5 scale using GPT-5-mini (Singh et al., 2025).

5 Results and Discussion

We execute a comprehensive evaluation of the SYNAPSE framework across a heterogeneous evaluation matrix of autoregressive decoders, directly contrasting open-weights architectures against proprietary commercial models hosted via

cloud inference endpoints. Translation fidelity is systematically analyzed using standard lexical overlap and embedding similarity protocols, paired with architectural ablation tracks designed to isolate the empirical impact of each neuro-symbolic module. Ultimately, these findings expose the dynamics of topological noise filtration, context grounding capacities, and computational efficiency profiles relative to contemporary brain-to-text configurations.

5.1 Quantitative Performance and Component Ablations

Under full deployment (\mathcal{A}_1), SYNAPSE establishes the premier performance tier across all decoders by unifying purified vocabulary vectors $\mathbf{W}_{\text{pruned}}$, relational knowledge blocks \mathcal{F} , and cross-modal syntactic templates $\mathcal{E}_{\text{exemplars}}$. A key structural insight emerges when evaluating the framework decoupled from its primary visual anchor (\mathcal{A}_4 , *w/o Perceptual Object Anchors*). In contemporary retrieval based pipelines like SENSE (Murhekar et al., 2026), removing visual class labels causes severe translation decay due to over-indexing on localized classifiers. Conversely, under SYNAPSE, withholding explicit object labels yields virtually no performance degradation; e.g., Qwen2.5-7B maintains a stable ROUGE-1 of 32.3 and BLEU-4 of 6.1. This directly validates the error-correction properties of our neuro-symbolic layer, which constructs a self-contained semantic landscape that shields generation from isolated encoder failures.

Systematic removal of subsequent pipeline layers highlights their distinct regularizing roles. Disabling explicit prose assertions (\mathcal{A}_5 , *w/o Relational Context Facts*) deprives the decoder of structured background knowledge \mathcal{F} , inducing stochastic approximation of semantic dependencies and immediate semantic drift. Deactivating cross-modal coordinate lookups (\mathcal{A}_4 , *w/o In-Context Exemplars*) forces a strict zero-shot stance, degrading sentence fluency due to the absence of the grammatical blueprint matrix $\mathcal{E}_{\text{exemplars}}$. Crucially, even the highly constrained configuration supplied exclusively with purified keywords (\mathcal{A}_6 , *Clean BoW Only*) consistently outperforms unaugmented contemporary benchmarks (SENSE) and fully fine-tuned THOUGHT2TEXT across matching architectural slices. This confirms that inference-time topological graph purification provides a fundamentally more resilient regularizer than unconstrained prompting or connectionist parameter updates.

| Ablation Configuration | | ROUGE | | R-L | BLEU | | MET. | BERT | GPT-5 Evaluation | | |
|---|---|-------------|------------|-------------|-------------|------------|-------------|-------------|------------------|-------------|--|
| ID | Decoder Model | R-1 | R-2 | | B-1 | B-4 | | Score | Fluency | Adequacy | |
| \mathcal{A}_1 (Full) | GPT-4o-mini | 31.7 | 8.8 | 28.1 | <u>27.6</u> | 5.9 | 28.2 | 90.2 | 4.79 | 1.37 | |
| | Gemini 2.5 Flash Lite | 32.3 | 8.6 | 28.6 | 27.3 | 5.8 | 27.5 | 90.3 | 4.68 | 1.37 | |
| | LLaMa-3-8B | 30.0 | 8.2 | 27.2 | 25.1 | 5.4 | 26.8 | 90.2 | 4.71 | 1.35 | |
| | Qwen2.5-7B | 32.2 | 9.3 | 28.7 | 27.3 | <u>6.1</u> | 28.0 | <u>90.4</u> | 4.48 | 1.35 | |
| \mathcal{A}_2 ($m = 0$) | GPT-4o-mini | 30.8 | 8.2 | 27.3 | 26.9 | 5.5 | 27.0 | 90.1 | 4.78 | 1.33 | |
| | Gemini 2.5 Flash Lite | 31.4 | 7.6 | 27.7 | 26.5 | 5.2 | 25.5 | 90.1 | 4.61 | 1.31 | |
| | LLaMa-3-8B | 29.5 | 7.9 | 26.8 | 24.6 | 5.2 | 26.1 | 90.1 | 4.69 | 1.33 | |
| | Qwen2.5-7B | 31.6 | 8.4 | 28.0 | 26.7 | 5.6 | 26.7 | 90.3 | 4.44 | 1.31 | |
| \mathcal{A}_3 (-Obj) | GPT-4o-mini | 31.6 | 8.7 | 27.9 | <u>27.6</u> | 5.9 | 28.2 | 90.2 | 4.78 | 1.36 | |
| | Gemini 2.5 Flash Lite | 32.3 | 8.4 | 28.4 | 27.4 | 5.7 | 27.4 | 90.3 | 4.64 | 1.35 | |
| | LLaMa-3-8B | 30.4 | 8.6 | 27.3 | 25.8 | 5.5 | 27.4 | 90.2 | 4.71 | 1.34 | |
| | Qwen2.5-7B | 32.3 | <u>9.2</u> | 28.6 | <u>27.6</u> | <u>6.1</u> | 28.2 | 90.3 | 4.38 | 1.34 | |
| \mathcal{A}_4 (-Exe) | GPT-4o-mini | 31.6 | 8.9 | 28.1 | <u>27.6</u> | 6.0 | 28.2 | 90.2 | 4.77 | 1.36 | |
| | Gemini 2.5 Flash Lite | 32.7 | 8.7 | 28.9 | 27.8 | 5.9 | 27.9 | 90.3 | 4.67 | 1.36 | |
| | LLaMa-3-8B | 29.8 | 8.2 | 27.1 | 25.0 | 5.4 | 26.7 | 90.2 | 4.72 | 1.36 | |
| | Qwen2.5-7B | 32.2 | 9.3 | 28.8 | 27.3 | <u>6.2</u> | 27.9 | <u>90.4</u> | 4.46 | 1.35 | |
| \mathcal{A}_5 (-Fac) | GPT-4o-mini | 30.9 | 8.2 | 27.3 | 26.9 | 5.5 | 28.0 | 90.0 | 4.78 | 1.35 | |
| | Gemini 2.5 Flash Lite | 32.3 | 8.4 | 28.3 | 27.8 | 5.6 | 28.0 | 90.2 | 4.66 | 1.34 | |
| | LLaMa-3-8B | 29.1 | 8.1 | 26.6 | 24.0 | 5.3 | 26.2 | 90.1 | 4.72 | 1.38 | |
| | Qwen2.5-7B | 32.0 | <u>9.2</u> | 28.6 | 26.8 | 6.2 | 26.9 | 90.5 | 4.57 | 1.36 | |
| \mathcal{A}_6 (Base) | GPT-4o-mini | 28.0 | 5.9 | 24.3 | 24.1 | 4.1 | 26.2 | 89.4 | 4.78 | 1.31 | |
| | Gemini 2.5 Flash Lite | 31.0 | 7.5 | 26.9 | 26.6 | 5.0 | 27.5 | 89.8 | 4.58 | 1.30 | |
| | LLaMa-3-8B | 25.3 | 5.3 | 21.6 | 21.4 | 3.5 | 24.8 | 89.1 | 4.46 | 1.25 | |
| | Qwen2.5-7B | 29.2 | 6.6 | 24.9 | 24.9 | 4.4 | 26.0 | 89.6 | 4.24 | 1.27 | |
| Baselines & Comparative Frameworks | | | | | | | | | | | |
| SENSE | GPT-4o-mini _{With Obj} | 30.6 | 8.2 | 28.2 | 24.9 | 5.6 | 25.3 | 89.8 | 4.75 | <u>1.40</u> | |
| | Gemini 2.5 Flash Lite _{With Obj} | 31.5 | 8.5 | 28.7 | 25.2 | 5.6 | 26.1 | 89.7 | 4.77 | <u>1.40</u> | |
| | LLaMa-3-8B _{With Obj} | 12.6 | 2.2 | 11.6 | 6.8 | 1.5 | 12.5 | 88.1 | 4.56 | 1.33 | |
| | Qwen2.5-7B _{With Obj} | 21.8 | 5.9 | 19.9 | 13.8 | 3.2 | 15.0 | 87.6 | 3.47 | 1.33 | |
| THOUGHT2TEXT | LLaMa-3-8B _{ALL} | 30.0 | 8.1 | 26.6 | 25.5 | 5.5 | 26.3 | 89.0 | 4.82 | 1.58 | |
| | Qwen2.5-7B _{ALL} | 26.4 | 4.6 | 22.8 | 22.7 | 3.7 | 21.1 | 88.0 | 4.75 | 1.28 | |

Table 1: Ablation tracking and comparative framework performance over the ImageNet-EEG benchmark. Higher values indicate superior performance across all metrics. Top results are **bolded** (tied **underlined**) and second-best are *italicized* (tied *underlined*). Setup configurations: \mathcal{A}_1 : Full framework; \mathcal{A}_2 : $m = 0$; \mathcal{A}_3 : Full w/o Object Labels; \mathcal{A}_4 : Full w/o Exemplars; \mathcal{A}_5 : Full w/o Facts; \mathcal{A}_6 : Minimal baseline (BoW + Obj only).

5.2 Characterizing Topological Incongruence and Pruning Dynamics

As hypothesized, filtering the singletons ($C_D(\mathbf{v}) = 0$) generated by *topical incongruence* establishes a deterministic error-correction barrier that halts noise propagation prior to LLM self-attention calculation. Parametric sensitivity sweeps over the priority safeguard hyperparameter $m \in \{0, 3, 5\}$ across both corpora expose distinct pruning trends (Table 2).

Our default configuration ($m = 5$) preserves an optimal balance on ImageNet-EEG, retaining a mean pool of 11.13 verified terms while filtering 3.87 words per trial (a 25.8% macro pruning rate). Removing the constraint ($m = 0$) drives macro dataset pruning to a 33.5% peak, scrubbing up to 13 words in highly corrupted intervals. While the

unconstrained filter aggressively minimizes biological noise, it introduces systemic vulnerabilities due to graph incompleteness, ruthlessly scrubbing valid visual descriptors that lack explicit common-sense paths within static databases.

Conversely, our connectivity constraint surfaces a vulnerability to *spurious relational co-activation*. If the connectionist frontend simultaneously triggers multiple incongruent noise words that share an explicit link in the knowledge base, they form an isolated noise subgraph. Because their individual degree metrics remain non-zero ($C_D(\mathbf{v}) > 0$), these anomalous terms bypass topological pruning entirely and leak into the prompt footprint. While our non-parametric blueprints $\mathcal{E}_{\text{exemplars}}$ and explicit facts cache \mathcal{F} insulate the decoder from crashing under these occasional leaks, this artifact

demonstrates that a permissive connectivity constraint safeguards rare, authentic neural intents at the cost of allowing clustered token noise to occasionally evade filtration.

Qualitative analysis (Appendix A) validates the synergy between our topological purification layer and language-model-driven semantic grounding. Table 4 reports the refined, pruned BoW inputs perceived by the decoder; notably, the system successfully resolves discordant noise via this dual-stage process. For instance, when the frontend emits spurious, isolated activations (e.g., *daisy*, *flower* for a target *mushroom*), the graph filter purges these structural outliers. By providing the LLM with these filtered tokens alongside grounded relational facts (\mathcal{F}), the decoder effectively ignores the residual noise to synthesize the correct target, demonstrating that disambiguation relies on both structural filtering and auxiliary semantic grounding. Conversely, Samples 5 and 6 reveal the framework’s operative limits: when noise tokens form a topologically consistent, coherent subgraph (e.g., a clustered co-activation of *pizza*, *pepperoni*, *cheese* for a *flower* stimulus), these terms retain centrality ($C_D(v) > 0$) and evade filtration. In such instances, the noise persists in the context window, forcing the decoder to negotiate structurally coherent but semantically incorrect inputs—a limitation that underscores our baseline reliance on frontend representation stability.

5.3 Neuro-Symbolic Decoupling vs. Fine-Tuning

End-to-end connectionist architectures typically optimize autoregressive weights directly on continuous features, assuming language decoders can naturally regularize transient bio-signal noise via gradient minimization. Our empirical metrics show this assumption fails under volatile, non-invasive recordings; uncorrected representation drift propagates unchecked, causing severe context pollution.

This representational vulnerability is acute within compact open-weights models (Meta-Llama-3-8B and Qwen2.5-7B). When subjected to unpurified retrieval matrices, these decoders suffer from severe *attentional dispersion*. The internal self-attention allocation grids must simultaneously filter a contextually contradictory token landscape and track long-range syntactic dependencies. This dual optimization dilutes the attention weight budget, preventing transformer layers from tracking a stable target distribution and

triggering context hallucinations.

SYNAPSE fundamentally alters this multi-modal dynamic by establishing a strict architectural separation of labor between perception and logic. By executing deterministic topological graph purification prior to prompt ingestion, our framework intercepts and purges signal noise before it pollutes the decoder’s input footprint. When conditioned exclusively on a validated token matrix $\mathbf{W}_{\text{pruned}}$, explicit prose assertions \mathcal{F} , and nearest-neighbor syntactic blueprints $\mathcal{E}_{\text{exemplars}}$, the downstream text generator can dedicate its entire attention allocation budget exclusively to linguistic synthesis and grammatical composition. Consequently, this modular neuro-symbolic division of labor insulates compact engines from attentional dispersion, enabling lightweight open-weights models to consistently match or exceed the translation precision of heavily fine-tuned, resource-intensive baselines.

5.4 Scaling and Cross-Dataset Constraints

To stress-test the architectural boundaries of SYNAPSE, we evaluate framework scaling over the large-scale THINGS EEG2 dataset (Table 3). Scaling from 40 to 1,654 semantic concepts induces high density inside the continuous feature space, causing significant latent cross-talk at the connectionist frontend. This systemic noise degradation explains the uniform compression of absolute metrics relative to ImageNet setups. This baseline friction is heavily compounded by our cross-exemplar zero-shot partitioning strategy; validating exclusively on the unseen 6th visual exemplar yields high representational volatility. This drops higher-order metrics uniformly across architectures, with BLEU-4 compressing from a baseline of ~ 6.0 down to ~ 3.0 .

Despite this dataset-level performance drop, the evaluation confirms the resilience of our symbolic intervention layer under high-density noise. Under the unaugmented SENSE baseline, the compact Qwen2.5-7B model suffers from catastrophic attentional dispersion, completely collapsing to 9.4 ROUGE-1 and 2.0 Fluency due to unpurified input vectors. Conversely, deploying the full SYNAPSE framework intercepts this noise, driving a dramatic recovery to 21.8 ROUGE-1 and 4.2 Fluency. This substantial recovery reinforces that as the connectionist perception frontend fractures under open-vocabulary scale, topological purification becomes increasingly vital to insulate compact language generators.

| Topological Filtration Metric | ImageNet-EEG | | Things EEG2 |
|---|-------------------|----------------|-------------|
| | $m = 5$ (Default) | $m = 0$ (None) | $m = 5$ |
| Average Retained Word Pool (words) | 11.13 | 9.98 | 11.41 |
| Average Dropped per Sample (words) | 3.87 | 5.02 | 3.59 |
| Macro Dataset Pruning Rate (%) | 25.8 | 33.5 | 23.9 |
| Maximum Dropped in a Single Trial (words) | 10 | 13 | 8 |

Table 2: Macro-level topological pruning and error-correction sensitivity statistics compared across the ImageNet-EEG ($N = 1, 987$) and Things EEG2 ($N = 1, 654$) datasets under variable priority safeguard constraints. For all evaluations, the minimum tokens dropped in a single trial was 0.

| Ablation ID | Configuration Decoder Model | ROUGE | | R-L | BLEU | | MET. | BERT Score | GPT-5 Evaluation | | |
|---|-----------------------------|-------------|------------|-------------|-------------|------------|-------------|-------------|------------------|-----|--|
| | | R-1 | R-2 | | B-1 | B-4 | | Fluency | Adequacy | | |
| \mathcal{B}_1 (Full) | GPT-4o-mini | 21.4 | 2.5 | 18.3 | 19.3 | 2.7 | 16.5 | 87.4 | 4.8 | 1.0 | |
| | Gemini 2.5 Flash Lite | 21.2 | 2.8 | 18.2 | 17.6 | 2.7 | 15.9 | 87.4 | 4.4 | 1.0 | |
| | LLaMa-3-8B | 20.3 | 3.9 | 18.3 | 17.8 | 3.0 | 17.1 | 87.4 | 4.5 | 1.0 | |
| | Qwen2.5-7B | 21.8 | 3.0 | 18.9 | 19.4 | 2.9 | 16.7 | 87.4 | 4.2 | 1.0 | |
| \mathcal{B}_2 (-Exe) | GPT-4o-mini | 21.1 | 2.1 | 18.1 | 18.4 | 2.5 | 15.9 | 87.4 | <u>4.7</u> | 1.0 | |
| | Gemini 2.5 Flash Lite | 21.4 | 2.4 | 18.4 | 18.5 | 2.7 | 16.3 | 87.2 | 4.3 | 1.0 | |
| | LLaMa-3-8B | 15.2 | 1.8 | 12.4 | 13.3 | 2.1 | 14.5 | 87.0 | 4.2 | 1.0 | |
| | Qwen2.5-7B | 21.5 | 2.5 | 18.1 | 19.4 | 2.7 | 16.8 | 87.0 | 3.9 | 1.0 | |
| Baselines & Comparative Frameworks | | | | | | | | | | | |
| SENSE (Base) | GPT-4o-mini | 21.2 | 2.7 | 19.4 | 13.4 | 2.1 | 14.1 | 88.5 | 4.8 | 1.0 | |
| | Gemini 2.5 Flash Lite | 22.5 | 4.2 | 21.2 | 13.2 | 2.4 | 15.1 | 88.2 | <u>4.7</u> | 1.0 | |
| | LLaMa-3-8B | 19.9 | 4.2 | 17.1 | 17.5 | 3.1 | 17.8 | 86.2 | 4.1 | 1.0 | |
| | Qwen2.5-7B | 9.4 | 1.2 | 8.5 | 3.6 | 0.7 | 4.3 | 84.7 | 2.0 | 1.0 | |

Table 3: Ablation tracking performance over the THINGS EEG2 cross-exemplar evaluation suite. Higher values indicate superior performance across all metrics. Setup configurations are explicitly mapped as follows: \mathcal{B}_1 : Full framework (BoW + Obj + Facts + Exemp); \mathcal{B}_2 : Full framework w/o Exemplars.

Finally, the experiment exposes a key trade-off concerning the cross-modal syntactic blueprint matrix ($\mathcal{E}_{\text{exemplars}}$). For compact open-weights architectures like Meta-LLaMa-3-8B, removing templates (*No Exemplars*) drops ROUGE-1 from 20.3 to 15.2, proving smaller models heavily rely on localized contextual patterns to structure output text. For high-capacity models like GPT-4o-mini, the marginal performance gap exposes a dataset limitation: the dense latent landscape can cause nearest-neighbor lookups to retrieve slightly displaced training exemplars, introducing mild stylistic constraints that distort the model’s unconstrained generation path. This indicates that while topological purification provides a critical baseline shield, future scaling will require dynamic scaling parameters to completely mitigate coordinate interference (see Appendix B for qualitative prompt details).

6 Conclusion

We introduced SYNAPSE, a lightweight neuro-symbolic framework for EEG-to-text decoding that stabilizes frozen language models through

inference-time symbolic regularization rather than resource-intensive end-to-end fine-tuning. By combining topological graph purification, relational grounding, and latent exemplar retrieval, SYNAPSE suppresses semantic drift and attentional dispersion caused by noisy neural projections. Experiments across multiple EEG benchmarks and heterogeneous LLM backends demonstrate consistent improvements over unconstrained prompting baselines, strong robustness under object-label ablation, and performance commensurate with substantially larger fine-tuned systems. More broadly, our findings suggest that brain-to-text decoding may benefit from a retrieval-augmented paradigm shift, where symbolic structure and external semantic memory stabilize generation without modifying model parameters. By externalizing semantic correction away from autoregressive weights and into structured inference-time retrieval, SYNAPSE offers a scalable, privacy-preserving, and computationally efficient direction for next-generation neuro-symbolic brain-computer interfaces.

7 Limitations

Despite the robustness gains introduced by SYNAPSE, several limitations remain. Non-invasive EEG recordings possess inherently low spatial resolution and remain highly susceptible to physiological noise, placing fundamental constraints on the fidelity of recovered semantic intent. While topological graph purification substantially reduces semantic drift and attentional dispersion, the framework still assumes that graph connectivity implies contextual validity; consequently, semantically incorrect but densely co-activated token clusters may occasionally evade pruning and propagate residual hallucinations into downstream generation. In addition, the effectiveness of symbolic regularization depends on the coverage and relational completeness of the external commonsense graph, which may omit rare or weakly connected visual concepts. The exemplar retrieval module is similarly constrained by static nearest-neighbor matching within dense latent neural embedding spaces, where semantically adjacent concepts can overlap under large-scale open-vocabulary settings. More broadly, SYNAPSE inherits a limitation common to retrieval-augmented paradigms: downstream generation quality remains fundamentally bounded by retrieval quality, which in our setting operates over noisy neural semantic projections rather than clean textual queries. Finally, although raw EEG processing and symbolic purification remain fully localized to preserve biometric privacy, several evaluated decoder backends rely on externally hosted LLM APIs, meaning full end-to-end privacy ultimately depends on deployment with fully local language models and on-device inference infrastructure.

8 Ethics Statement

SYNAPSE is designed as a lightweight and privacy-conscious framework for EEG-to-text decoding, with the goal of supporting assistive communication technologies for individuals affected by neurological impairments. The architecture performs neural feature extraction and symbolic regularization entirely within the local device boundary, ensuring that raw brain signals are never transmitted to external inference services and thereby reducing risks associated with sensitive biometric exposure. To minimize ungrounded or hallucinated text generation, SYNAPSE incorporates explicit semantic regularization through topological graph

purification and constrained vocabulary grounding. Additionally, the framework operates using generalized neural alignment representations without requiring subject-specific fine-tuning, promoting broader accessibility and reducing dependence on individualized calibration. We emphasize user privacy, transparent inference, and responsible deployment throughout the design of the system. We utilize the ConceptNet knowledge graph under its Creative Commons Attribution-ShareAlike 4.0 license and adhere to the usage terms for the publicly available EEG benchmarks used in our training pipeline.

9 Potential Risks

While SYNAPSE is developed strictly for assistive communication, we acknowledge the inherent dual-use nature of brain-computer interface (BCI) technologies. The ability to decode neural activity into semantic concepts could theoretically be repurposed for non-consensual cognitive monitoring or unauthorized neural profiling. To mitigate these risks, our research framework intentionally constrains the decoding process to perceived visual stimuli rather than internal thoughts or emotive states. Furthermore, by strictly localizing all neural processing to the user’s device—thereby eliminating the need to transmit raw brain data to cloud services—we prioritize individual autonomy and data sovereignty as fundamental safeguards against the potential misuse of neural decoding technology.

Generative AI Disclosure

Generative AI tools, including ChatGPT and Gemini, were used during manuscript preparation to assist with \LaTeX formatting, language refinement, conciseness, and debugging support. All authors carefully reviewed, edited, and take full responsibility for the final manuscript content.

References

- Josh Achiam, Steven Adler, Sandhini Agarwal, Lama Ahmad, Ilge Akkaya, Florencia Leoni Aleman, Diogo Almeida, Janko Altschmidt, Sam Altman, Shyamal Anadkat, and 1 others. 2023. Gpt-4 technical report. *arXiv preprint arXiv:2303.08774*.
- Satanjeev Banerjee and Alon Lavie. 2005. Meteor: An automatic metric for mt evaluation with improved correlation with human judgments. In *Proceedings of the acl workshop on intrinsic and extrinsic evaluation measures for machine translation and/or summarization*, pages 65–72.
- Yohann Benchetrit, Hubert Banville, and Jean-Rémi King. 2023. Brain decoding: toward real-time reconstruction of visual perception. *arXiv preprint arXiv:2310.19812*.
- Alexandre Défossez, Charlotte Caucheteux, Jérémy Rapin, Ori Kabeli, and Jean-Rémi King. 2023. Decoding speech perception from non-invasive brain recordings. *Nature Machine Intelligence*, 5(10):1097–1107.
- Alessandro T Gifford, Kshitij Dwivedi, Gemma Roig, and Radoslaw M Cichy. 2022. A large and rich eeg dataset for modeling human visual object recognition. *NeuroImage*, 264:119754.
- Bin He, Bryan Baxter, Bradley J Edelman, Christopher C Cline, and W Ye Wenjing. 2015. Noninvasive brain-computer interfaces based on sensorimotor rhythms. *Proceedings of the IEEE*, 103(6):907–925.
- Zenon Lamprou and Yashar Moshfeghi. 2025. On creating a brain-to-text decoder. *arXiv preprint arXiv:2501.06326*.
- Jarod Lévy, Mingfang Zhang, Svetlana Pinet, Jérémy Rapin, Hubert Banville, Stéphane d’Ascoli, and Jean-Rémi King. 2025. Brain-to-text decoding: A non-invasive approach via typing. *arXiv preprint arXiv:2502.17480*.
- Chin-Yew Lin. 2004. Rouge: A package for automatic evaluation of summaries. In *Text summarization branches out*, pages 74–81.
- Xiaozhao Liu, Dinggang Shen, and Xihui Liu. 2025. Learning interpretable representations leads to semantically faithful eeg-to-text generation. *arXiv preprint arXiv:2505.17099*.
- Mohamed Masry, Mohamed Amen, Mohamed Elzyat, Mohamed Hamed, Norhan Magdy, and Maram Khaled. 2025. Ets: Open vocabulary electroencephalography-to-text decoding and sentiment classification. *arXiv preprint arXiv:2506.14783*.
- Sean L Metzger, Jessie R Liu, David A Moses, Maximilian E Dougherty, Margaret P Seaton, Kaylo T Littlejohn, Josh Chartier, Gopala K Anumanchipalli, Adelyn Tu-Chan, Karunesh Ganguly, and 1 others. 2022. Generalizable spelling using a speech neuro-prosthesis in an individual with severe limb and vocal paralysis. *Nature communications*, 13(1):6510.
- Abhijit Mishra, Shreya Shukla, Jose Torres, Jacek Gwizdka, and Shounak Roychowdhury. 2025. Thought2Text: Text generation from EEG signal using large language models (LLMs). In *Findings of the Association for Computational Linguistics: NAACL 2025*, pages 3747–3759, Albuquerque, New Mexico. Association for Computational Linguistics.
- Akshaj Murhekar, Christina Liu, Abhijit Mishra, Shounak Roychowdhury, and Jacek Gwizdka. 2026. Sense: Efficient eeg-to-text via privacy-preserving semantic retrieval. *Preprint*, arXiv:2603.17109.
- Kishore Papineni, Salim Roukos, Todd Ward, and Wei-Jing Zhu. 2002. Bleu: a method for automatic evaluation of machine translation. In *Proceedings of the 40th annual meeting of the Association for Computational Linguistics*, pages 311–318.
- Aaditya Singh, Adam Fry, Adam Perelman, Adam Tart, Adi Ganesh, Ahmed El-Kishky, Aidan McLaughlin, Aiden Low, AJ Ostrow, Akhila Ananthram, Akshay Nathan, Alan Luo, Alec Helyar, Aleksander Madry, Aleksandr Efremov, Aleksandra Spyra, Alex Baker-Whitcomb, Alex Beutel, Alex Karpenko, and 465 others. 2025. Openai gpt-5 system card. *Preprint*, arXiv:2601.03267.
- Concetto Spampinato, Simone Palazzo, Isaak Kavasidis, Daniela Giordano, Nasim Souly, and Mubarak Shah. 2017. Deep learning human mind for automated visual classification. In *Proceedings of the IEEE conference on computer vision and pattern recognition*, pages 6809–6817.
- Robyn Speer, Joshua Chin, and Catherine Havasi. 2017. Conceptnet 5.5: an open multilingual graph of general knowledge. In *Proceedings of the Thirty-First AAAI Conference on Artificial Intelligence, AAAI’17*, page 4444–4451. AAAI Press.
- Jerry Tang, Amanda LeBel, Shailee Jain, and Alexander G Huth. 2023. Semantic reconstruction of continuous language from non-invasive brain recordings. *Nature Neuroscience*, 26(5):858–866.
- Yitian Tao, Yan Liang, Luoyu Wang, Yongqing Li, Qing Yang, and Han Zhang. 2025. See: Semantically aligned eeg-to-text translation. In *ICASSP 2025-2025 IEEE International Conference on Acoustics, Speech and Signal Processing (ICASSP)*, pages 1–5. IEEE.
- Hugo Touvron, Thibaut Lavril, Gautier Izacard, Xavier Martinet, Marie-Anne Lachaux, Timothée Lacroix, Baptiste Rozière, Naman Goyal, Eric Hambro, Faisal Azhar, and 1 others. 2023. Llama: Open and efficient foundation language models. *arXiv preprint arXiv:2302.13971*.
- Jiaqi Wang, Zhenxi Song, Zhengyu Ma, Xipeng Qiu, Min Zhang, and Zhiguo Zhang. 2024. Enhancing

eeg-to-text decoding through transferable representations from pre-trained contrastive eeg-text masked autoencoder. In *Proceedings of the 62nd Annual Meeting of the Association for Computational Linguistics (Volume 1: Long Papers)*, pages 7278–7292.

Francis R Willett, Erin M Kunz, Chaofei Fan, Donald T Avansino, Guy H Wilson, Eun Young Choi, Foram Kamdar, Matthew F Glasser, Leigh R Hochberg, Shaul Druckmann, and 1 others. 2023. A high-performance speech neuroprosthesis. *Nature*, 620(7976):1031–1036.

Haitao Wu, Qing Li, Changqing Zhang, Zhen He, and Xiaomin Ying. 2025. Bridging the vision-brain gap with an uncertainty-aware blur prior. In *Proceedings of the IEEE/CVF Conference on Computer Vision and Pattern Recognition (CVPR)*.

Tianyi Zhang, Varsha Kishore, Felix Wu, Kilian Q Weinberger, and Yoav Artzi. 2019. Bertscore: Evaluating text generation with bert. *arXiv preprint arXiv:1904.09675*.

A Qualitative Generation Examples

This appendix provides a representative suite of translated natural language sentences generated from non-invasive biological signal features, demonstrating the semantic error-correction capabilities of our framework.









| ID | Image | Ref. Obj | Pred. Obj | Reference Description | Thought2Text | Pruned BoW | SYNAPSE Description |
|----|---|------------|------------|---|--|--|---|
| 1 |  | mushroom | mushroom | A large yellow mushroom with a brown stem and a brown cap, surrounded by green foliage. | A group of mushrooms growing on a log. | yellow, mushroom, white, daisy, flower, grow, green forest | A yellow mushroom growing in a green forest. |
| 2 |  | piano | piano | A black grand piano in a living room. | A grand piano with a stool in front of it. | piano, black, room, grand, wooden, floor | A black grand piano in a room with a wooden floor and chair. |
| 3 |  | camping | camping | A tent in a mountainous area with trees and fog. | A tent set up in a forest with a campfire nearby. | tent, white, blue, mountains, field, area | Two green tents in a grassy field with mountains in the background. |
| 4 |  | pumpkin | pumpkin | A carved pumpkin with a face and eyes, sitting on a table. | A carved pumpkin with a spooky face on it. | carved, pumpkin, face, carving, spooky | A carved pumpkin with a jack-o-lantern face. |
| 5 |  | flower | mushroom | A black and white photograph of a single daisy with a white center and a dark brown center. | A group of mushrooms growing on a log. | pizza, mushroom, pepperoni, cheese, white, yellow | A pizza with mushrooms and cheese on a white table. |
| 6 |  | coffee mug | coffee mug | A hand holding a mug with a blue background and a handprint design. | A person holding a coffee mug with the words "World's Best Dad" written on it. | car, convertible, mug, green, coffee, vehicle | A green convertible driving on the street with a white coffee mug on the dashboard. |
| 7 |  | guitar | train | A young boy sitting on a chair playing a guitar. | A man is holding a guitar in front of a microphone. | train, track, black, blue, white, red, station | A train on a track at a station, red and black. |
| 8 |  | piano | ball | A man in a red coat and black pants is playing a piano in a room with a chandelier. | A man is playing the piano in a dimly lit room. | piano, golf, ball, black, room, white, floor, orchestra | A man standing in a room with black floor, playing a piano at an orchestra while golf balls are nearby. |

Table 4: Qualitative comparison of generated descriptions from SYNAPSE and the THOUGHT2TEXT baseline. The Pruned BoW column details the resultant pruned token footprint after the topological graph refining phase is completed, *captions generated by Qwen2.5-7B*.

B Inference-Time Prompt Blueprints

To guarantee reproducibility across inference endpoints, we detail the prompt layouts generated by the SYNAPSE framework.

B.1 ImageNet Evaluation Profiles

B.1.1 Main Production Architecture (Full Graph RAG Augmentation)

This blueprint represents configuration \mathcal{A}_1 , delivering the full consolidated neuro-symbolic payload—including topologically pruned vocabulary vectors $\mathbf{W}_{\text{pruned}}$, grounded relational knowledge blocks \mathcal{F} , cross-modal syntactic templates $\mathcal{E}_{\text{exemplars}}$, and continuous perceptual classification metrics—to the language decoder.

You are an advanced neural decoding translation engine. You are provided with a denoised, common-sense validated Bag-of-Words extracted from human EEG signals, along with topological world constraints and structural sentence guidelines. Your task is to synthesize these primitives into a single natural description.

[Structural Layout Guides from Training Set]
{retrieved_exemplars}

[Denoised Brain-Signal Keywords]
[{\prompt_words}]

[Topological Common-Sense Relations]
{relational_facts}

[Target Dominant Signal Context]
- Primary Classification Target: '{pred_obj}' (Model Confidence: {pred_conf})

Instructions:

1. Synthesize these primitives into exactly ONE clear, fluent English description (8-20 words).
2. Prioritize concepts verified by both the brain-signal keywords and the common-sense relational constraints.
3. Do NOT include annotations, prefix strings, quotes, or conversational meta-commentary. Output ONLY the raw caption string text.

Output:

B.1.2 Graph Cleaned Bag-of-Words Minimal Baseline (\mathcal{A}_6)

This configuration isolates the base limits of our network-filtering mechanism, conditioning the decoder exclusively on the degree centrality filtered keywords alongside standard classification arrays.

You are an advanced neural decoding translation engine. You are provided with a denoised, common-sense validated Bag-of-Words extracted from human EEG signals. Your task is to synthesize these primitives into a single natural description.

[Denoised Brain-Signal Keywords]
[{\prompt_words}]

[Target Dominant Signal Context]
- Primary Classification Target: '{pred_obj}' (Model Confidence: {pred_conf})

Instructions:

1. Synthesize these primitives into exactly ONE clear, fluent English description (8-20 words).
2. Prioritize concepts verified by the brain-signal keywords.
3. Do NOT include annotations, prefix strings, quotes, or conversational meta-commentary. Output ONLY the raw caption string text.

Output:

B.1.3 Context Resilience Prompt Track (\mathcal{A}_3)

Designed to measure framework vulnerability to isolated connectionist failures, this configuration decouples the generation sequence from primary perceptual tracking classes, relying on the residual symbolic landscape.

You are an advanced neural decoding translation engine. You are provided with a denoised, common-sense validated Bag-of-Words extracted from human EEG signals, along with topological world constraints and structural sentence guidelines. Your task is to synthesize these primitives into a single natural description.

[Structural Layout Guides from Training Set]

{retrieved_exemplars}

[Denoised Brain-Signal Keywords]

[{prompt_words}]

[Topological Common-Sense Relations]

{relational_facts}

Instructions:

1. Synthesize these primitives into exactly ONE clear, fluent English description (8-20 words).
2. Prioritize concepts verified by both the brain-signal keywords and the common-sense relational constraints.
3. Do NOT include annotations, prefix strings, quotes, or conversational meta-commentary. Output ONLY the raw caption string text.

Output:

B.1.4 Relational Fact Ablation Configuration (\mathcal{A}_5)

This template deactivates the relational background constraints cache \mathcal{F} . It forces the autoregressive layers to process structural layout guides and keyword vectors without explicit common-sense grounding linkages.

You are an advanced neural decoding translation engine. You are provided with a denoised, common-sense validated Bag-of-Words extracted from human EEG signals, along with structural sentence guidelines. Your task is to synthesize these primitives into a single natural description.

[Denoised Brain-Signal Keywords]

[{prompt_words}]

[Structural Layout Guides from Training Set]

{retrieved_exemplars}

[Target Dominant Signal Context]

- Primary Classification Target: '{pred_obj}' (Model Confidence: {pred_conf})

Instructions:

1. Synthesize these primitives into exactly ONE clear, fluent English description (8-20 words).
2. Prioritize concepts verified by both the brain-signal keywords and the common-sense relational constraints.
3. Do NOT include annotations, prefix strings, quotes, or conversational meta-commentary. Output ONLY the raw caption string text.

Output:

B.1.5 In-Context Exemplar Blueprint Ablation Configuration (\mathcal{A}_4)

This setting isolates model reactions to a strict zero-shot operational setting by dropping the grammatical blueprint matrix $\mathcal{E}_{\text{exemplars}}$ while preserving connectionist and relational anchors.

You are an advanced neural decoding translation engine. You are provided with a denoised, common-sense validated Bag-of-Words extracted from human EEG signals, along with topological world constraints. Your task is to synthesize these primitives into a single natural description.

[Denoised Brain-Signal Keywords]

[{prompt_words}]

[Topological Common-Sense Relations]

{relational_facts}

[Target Dominant Signal Context]

- Primary Classification Target: '{pred_obj}' (Model Confidence: {pred_conf})

Instructions:

1. Synthesize these primitives into exactly ONE clear, fluent English description (8-20 words).
2. Prioritize concepts verified by both the brain-signal keywords and the common-sense relational constraints.
3. Do NOT include annotations, prefix strings, quotes, or conversational meta-commentary. Output ONLY the raw caption string text.

Output:

B.2 THINGS EEG2 Scaling Profiles

To trace the scaling dynamics within the experimental scope, we document the prompting profiles configured for the multi-subject THINGS EEG2 matrix.

B.2.1 THINGS EEG2 Full Scaling Model Architecture (\mathcal{B}_1)

This prompt represents the active baseline configuration for the THINGS EEG2 task, tracking multi-class alignments over the vast candidate universe by aggregating the filtered token matrix alongside structural nearest-neighbor training vectors.

You are an advanced neural decoding translation engine. You are provided with a denoised, common-sense validated Bag-of-Words extracted from human EEG signals, along with topological world constraints and exemplar captions from similar samples from training data. Your task is to synthesize these primitives into a single natural description.

[Denoised Brain-Signal Keywords]
[`{words_str}`]

[Topological Common-Sense Relations]
`{facts_str}`

[Retrieved Exemplars]
`{exemplars_str}`

Instructions:

1. Synthesize these primitives into exactly ONE clear, fluent English description (8-20 words).
2. Prioritize concepts verified by both the brain-signal keywords and the common-sense relational constraints.
3. Do NOT include annotations, prefix strings, quotes, or conversational meta-commentary. Output ONLY the raw caption string text.

Output:

B.2.2 THINGS EEG2 Syntactic Blueprint Matrix Ablation (\mathcal{B}_2)

This template strips away cross-modal target coordinates ($\mathcal{E}_{\text{exemplars}}$), forcing the autoregressive decoder to structure descriptions under high crowding metrics without localized sentence templates.

You are an advanced neural decoding translation engine. You are provided with a denoised, common-sense validated Bag-of-Words extracted from human EEG signals, along with topological world constraints. Your task is to synthesize these primitives into a single natural description.

[Denoised Brain-Signal Keywords]
[`{words_str}`]

[Topological Common-Sense Relations]
`{facts_str}`

Instructions:

1. Synthesize these primitives into exactly ONE clear, fluent English description (8-20 words).
2. Prioritize concepts verified by both the brain-signal keywords and the common-sense relational constraints.
3. Do NOT include annotations, prefix strings, quotes, or conversational meta-commentary. Output ONLY the raw caption string text.

Output: